Modulation of transcriptional burst frequency by histone acetylation

Damien Nicolas[a], Benjamin Zoller[a], David M. Suter[a], and Felix Naef[a,1]

[a]Institute of Bioengineering, School of Life Sciences, Ecole Polytechnique Fédérale de Lausanne, Lausanne CH-1015, Switzerland

Edited by Joseph S. Takahashi, Howard Hughes Medical Institute and University of Texas Southwestern Medical Center, Dallas, TX, and approved May 21, 2018 (received for review December 22, 2017)

Many mammalian genes are transcribed during short bursts of variable frequencies and sizes that substantially contribute to cell-to-cell variability. However, which molecular mechanisms determine bursting properties remains unclear. To probe putative mechanisms, we combined temporal analysis of transcription along the circadian cycle with multiple genomic reporter integrations, using both short-lived luciferase live microscopy and single-molecule RNA-FISH. Using the *Bmal1* circadian promoter as our model, we observed that rhythmic transcription resulted predominantly from variations in burst frequency, while the genomic position changed the burst size. Thus, burst frequency and size independently modulated *Bmal1* transcription. We then found that promoter histone-acetylation level covaried with burst frequency, being greatest at peak expression and lowest at trough expression, while remaining unaffected by the genomic location. In addition, specific deletions of ROR-responsive elements led to constitutively elevated histone acetylation and burst frequency. We then investigated the suggested link between histone acetylation and burst frequency by dCas9p300-targeted modulation of histone acetylation, revealing that acetylation levels influence burst frequency more than burst size. The correlation between acetylation levels at the promoter and burst frequency was also observed in endogenous circadian genes and in embryonic stem cell fate genes. Thus, our data suggest that histone acetylation-mediated control of transcription burst frequency is a common mechanism to control mammalian gene expression.

transcriptional bursting | stochastic gene expression | histone acetylation | circadian oscillator | *Bmal1*

In higher eukaryotes, gene transcription in individual cells is intrinsically stochastic (1, 2). In particular, in many genes, RNA synthesis is subject to a pulsatile pattern and occurs mainly during short, often intense periods known as transcriptional bursts, followed by longer periods of transcription inactivity (3–5). The transcriptional bursting behavior of a gene is typically described by its burst frequency (i.e., the number of bursts in time units) and burst size (i.e., the mean number of transcripts produced per burst episode). Interestingly, these bursting kinetics are highly gene-specific (5–8) and likely reflect the complexity of regulatory mechanisms underlying gene expression and the diversity of molecular events participating in tuning transcription.

Recent studies aimed at understanding how burst frequencies and sizes are controlled (9). In particular, burst frequency is able to tune gene expression and is sensitive to concentration of transcription factors (10–13). Possibly linked to transcription factor binding, DNA loops between distal regulatory elements and the promoter also predominantly influence burst frequency (14–16). Furthermore, nucleosome clearance around transcription start sites (TSSs) modulate burst frequency, which is anti-correlated with nucleosome occupancy in both yeast cells (17, 18) and mammalian cells (19). In contrast, other variables, such as the number and affinity of DNA regulatory elements on gene promoters, influence the burst size (5, 11). Finally, how the chromatin context modulates transcriptional bursting remains controversial, as both genomic position and enrichment of specific histone marks have been shown to influence burst frequency, burst size, or both (5, 10, 19–21).

In the present study, we further dissected how the control of gene expression is implemented on the level of transcriptional bursting parameters, particularly burst frequency and size. To address this, we exploited two opportunities: the possibility of monitoring periodically changing gene expression levels during the endogenously ticking circadian cycle, and using genome engineering to insert reporters at different genomic locations. By focusing on transcriptional bursting of the *Bmal1* promoter driving a short-lived luciferase reporter, we found that burst frequency was accompanied by and directly influenced by promoter acetylation. This link between histone acetylation and burst frequency was also observed in endogenous circadian genes expressed at different times and in stem cell genes. Thus, we have found that histone acetylation increases transcription burst frequency, a mechanism that appears to modulate transcription in various mammalian systems.

Results

Live Analysis of *Bmal1* Transcription Shows That Genomic Location and Circadian Time Modulate Burst Size and Frequency. To monitor transcriptional bursting of *Bmal1* over the circadian cycle, we used a destabilized luciferase reporter with transcript and protein half-lives of 60 and 22 min, respectively (*SI Appendix*, Fig. S1*A*), allowing estimation of transcriptional bursting from single-cell luminescence traces (5, 22, 23). This reporter, hereinafter referred as *Bmal1-sLuc2*, was stably integrated by FRT recombination as a single copy in the genome of NIH 3T3 fibroblasts (Fig. 1*A*), and three clones differing in their reporter integration site were selected (*SI Appendix*, Fig. S1*B*). While after synchronization, all three clones displayed robust oscillations in luciferase expression at

Significance

Single-cell approaches have shown that many mammalian genes are transcribed stochastically in bursts of specific sizes and frequencies; however, molecular mechanisms controlling these bursting parameters have remained largely undetermined. By studying transcriptional bursting of a luciferase reporter controlled by a circadian gene promoter, we found that the gene integration site mainly influenced the burst size, while the circadian time primarily modulated the burst frequency. These daily variations in burst frequency correlated with histone acetylation levels, and CRISPR-Cas9–mediated acetylation of the promoter was sufficient to change the burst frequency. Since this correlation was also observed in other genes and in several cell types, we conclude that the impact of histone acetylation on gene expression is achieved mainly through modulation of burst frequency.

Author contributions: D.N., D.M.S., and F.N. designed research; D.N. and B.Z. performed research; D.N. and B.Z. analyzed data; and D.N., B.Z., and F.N. wrote the paper.

The authors declare no conflict of interest.

This article is a PNAS Direct Submission.

[1]To whom correspondence should be addressed. Email: felix.naef@epfl.ch.

This article contains supporting information online at www.pnas.org/lookup/suppl/doi:10.1073/pnas.1722330115/-/DCSupplemental.

Published online June 18, 2018.

SYSTEMS BIOLOGY

the population level, the reporter integration site significantly influenced the mean expression levels (Fig. 1*B*). Namely, the clone with the highest expression (clone H) globally exhibited a 2.5-fold greater signal than the medium expression clone (clone M) and a 3-fold greater signal than the lowest expression clone (clone L).

For the three clones, luminescence signals were also monitored at the single-cell level with a 5-min time resolution, as described previously (5, 22, 23). While individual cells displayed heterogeneous temporal signals (Fig. 1*C*), the averaged traces accurately reproduced the population luminescence (*SI Appendix*, Fig. S2*A*). These single-cell traces were then used to estimate the transcriptional bursting parameters for each clone along the circadian cycle by adapting an inference approach based on the two-state telegraph model (*SI Appendix*, Fig. S2*B*) (5, 23). Specifically, we applied a sliding window to independently analyze trace sections of 8 h, sliding every 4 h. From this, the inferred *Bmal1-sLuc2* mRNA copy numbers (ranging from 2 to 20) showed rhythmicity in all three clones (Fig. 1*D*). The underlying burst frequencies showed clear rhythms with a similar phase as mRNA accumulation for all clones (Fig. 1*E*), which arose mainly from longer promoter off-times during the expression trough (*SI Appendix*, Fig. S2*C*). Strikingly, the burst frequencies were comparable among the clones, indicating little influence from the reporter integration site. On the other hand, the burst sizes displayed less variability between the time points and did not exhibit clear circadian variations despite a global decrease after 22 h. Moreover, the burst size was markedly higher in the most highly expressing clone (Fig. 1*F*). Thus, these data suggest that for *Bmal1-sLuc2*, temporal variations in transcriptional output over the circadian period arose mainly from rhythmic burst frequency, while expression variations among the clones could be explained by differences in burst sizes. By measuring the expression levels of endogenous circadian genes, we verified that these differences in burst size corresponding to different reporter integration sites were not clonal effects (*SI Appendix*, Fig. S3*A*).

Single-Molecule RNA-FISH Recapitulates Real-Time mRNA Distributions and Bursting Parameters. To validate these results and quantify the number of *Bmal1-sLuc2* transcripts per cell, we performed single-molecule RNA-FISH (smRNA-FISH) with probes specifically targeting the intronless luciferase mRNA (Fig. 2*A*). *Bmal1-sLuc2* mRNA distributions measured with smRNA-FISH in the H, M, and L clones fit remarkably well with those inferred from the live analysis (*SI Appendix*, Fig. S3*B*). We then assessed the number of *Bmal1-sLuc2* transcripts per cell for all three clones at 16 h and 28 h after dexamethasone (dex) synchronization (*SI Appendix*, Fig. S3*C*), corresponding to the respective peak and trough accumulation times (*SI Appendix*, Fig. S3 *D* and *E*). Following previous work (4, 19), we fitted a negative binomial distribution to assess the burst size and frequency (in units of mRNA lifespan) from the smRNA-FISH distributions (Fig. 2*B*). Although amplitudes between peaks and troughs were less pronounced (Fig. 2*C*), smRNA-FISH confirmed that burst frequency was greatest at peak expression (significant differences in the H and L clones), while burst size did not change (Fig. 2 *D* and *E*). Moreover, the higher mean mRNA expression levels of the H clone compared with the M and L clones arose from the differences in burst sizes, showing similar values in the smRNA-FISH and live approaches (Fig. 2*E*). Thus, these smRNA-FISH data support the changes in transcriptional bursting parameters across time and insertion sites obtained from real-time luminescence.

Rhythmic Histone Acetylation at the *Bmal1* Promoter Correlates with Variations in Bursting Frequency, but Not with Burst Size. Both single-cell luminescence and smRNA-FISH showed that while the reporter integration site affected expression levels through variations of the burst size, the circadian time primarily modulated the burst frequency in each clone. Thus, the burst size and frequency are uncoupled and likely involve specific molecular mechanisms to modulate gene expression. We sought to identify mechanisms that could explain the temporal variations in burst frequency of *Bmal1-sLuc2*. Previous work showed that the circadian expression of *Bmal1* is controlled by two ROR-responsive elements (ROREs) at the TSS that rhythmically recruit the ROR family of activators and REV-ERB repressors (24, 25). Due to the phase-specific recruitment of NCoR and HDAC3 corepressive complexes (26), the promoter of *Bmal1* is rhythmically acetylated over the circadian period (27).

To assess whether the *Bmal1-sLuc2* acetylation state and burst frequency are linked, we quantified the H3K27ac levels of the reporter promoter at the expression peak and trough by chromatin immunoprecipitation (ChIP). In each clone, acetylation levels at *Bmal1-sLuc2* promoter were significantly enriched at the expression peak, as for the endogenous *Bmal1* locus, but not for the arrhythmic *Cyclophilin B* gene (Fig. 3*A*). However, H3K27ac levels remained comparable between the clones. Thus, *Bmal1-sLuc2* promoter acetylation covaried with modulation of the burst frequency; both quantities were unaffected by the integration site and varied with circadian time.

We further confirmed the correlation between *Bmal1-sLuc2* histone acetylation and burst frequency by generating a mutated *Bmal1* reporter lacking the two RORE and thus unable to recruit RORs and REV-ERBs (*SI Appendix*, Fig. S4*A*) (25, 28). After stable integration in the genomic FRT site of the H, the ΔRORE *Bmal1-sLuc2* reporter abrogated the rhythmic expression pattern of the WT promoter by maintaining the expression level close to the circadian peak (Fig. 3*B*), suggesting that REV-ERB–mediated repression dominates the circadian regulation of the stably integrated *Bmal1* reporter. In addition, this expression profile resembled that of a drug-mediated hyperacetylated reporter (*SI Appendix*, Fig. S4*B*). Indeed, mutations of the RORE led to constitutively

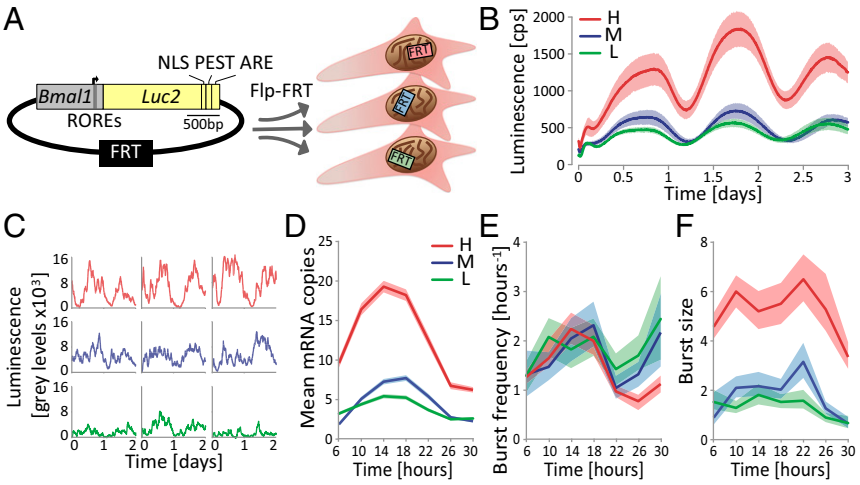

Fig. 1. Live analysis of *Bmal1* transcription showing that genomic location and circadian time modulate burst size and frequency, respectively. (*A*) Integration of a single copy of a *Bmal1-sLuc2* reporter at three genomic locations using Flp-FRT recombination. The *Bmal1* promoter (gray) contains two RORE (dark gray), and the *Luc2* coding sequence (yellow) includes an NLS, a PEST, and an ARE for protein and mRNA destabilization (5). (*B*) Real-time luminescence recordings of *Bmal1-sLuc2* in populations of H (high), M (medium), and L (low) clones. Data are mean ± SD over three replicates. (*C*) Examples of single-cell luminescence traces of the H, M, and L clones. (*D*–*F*) *Bmal1-sLuc2* transcriptional bursting parameters—mean mRNA copies per cell (*D*), burst frequency (*E*), and burst size (*F*)—inferred from single-cell luminescence traces of the H, M, and L clones. Data are mean and 95% CI of the posterior distribution.

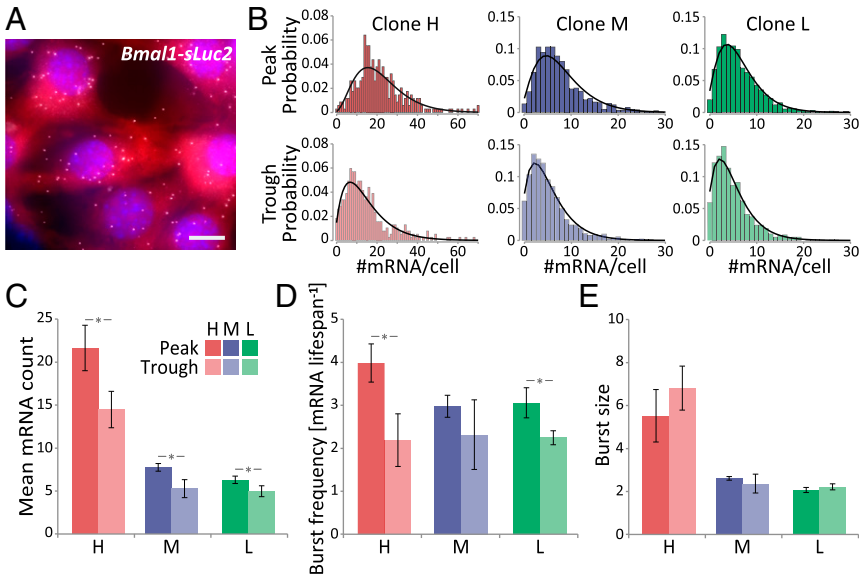

Fig. 2. Analysis of transcriptional bursting by smRNA-FISH recapitulating real-time bursting parameters. (*A*) smRNA-FISH detection of *Bmal1-sLuc2* transcripts in the H clone at 16 h after dex synchronization. Nuclei are stained with DAPI (blue), and cells are stained with HCS CellMask (red). (Scale bar: 10 μm.) (*B*) Pooled smRNA-FISH distributions of *Bmal1-sLuc2* transcripts in triplicate of the H, M, and L clones at 16 h (peak) and 28 h (trough) after synchronization, overlaid with negative binomial fits (black curve). Information on mRNA distributions and negative binomial fits of individual replicates is provided in *SI Appendix*, Table S3. (*C*–*E*) Transcriptional bursting parameters inferred from negative binomial fits on smRNA-FISH distributions. Mean mRNA count per cell (*C*), burst frequency (*D*), and burst size (*E*) are shown as mean ± SD over three replicates. $*P < 0.05$, *t* test.

elevated levels of H3K27ac specifically at the *Bmal1-sLuc2* reporter (Fig. 3*A*). We then used single-cell luminescence traces to infer the transcriptional bursting parameters of WT or ΔRORE reporters around the times of peak and trough expression. As before in the H clone (Fig. 1*E*), circadian variations in the expression of the WT *Bmal1-sLuc2* could be explained mainly by changes in burst frequency (Fig. 3*C*), although the burst size was greater in these data (*Discussion*). In the double-ΔRORE mutant cells, however, the transcriptional bursting parameters remained unchanged between peak and trough despite lower absolute burst size and higher frequency (both by approximately 1.4-fold) compared with the WT measurements at the peak. Thus, the ROREs in the *Bmal1-sLuc2* promoter were required for the drop in burst frequency at the expression trough. Taken together, these results suggest that *Bmal1-sLuc2* burst frequency is correlated with histone acetylation state. Indeed, the two covary along circadian time while remaining constant between the clones. In addition, the two ROREs responsible for rhythmic acetylation of the *Bmal1* promoter modulate bursting frequency, but not burst size.

We next searched for chromatin features that might explain the differences in burst size among the clones. None of the four chromatin marks that we measured by ChIP at the *Bmal1-sLuc2* promoter for the three clones H, M, and L was correlated with burst size (*SI Appendix*, Fig. S5*A*). Similarly, a set of published chromatin marks quantified at the reporter integration sites did not reveal significant associations with burst size (*SI Appendix*, Fig. S5*B*).

Histone Acetylation Levels at the *Bmal1-sLuc2* Promoter Determine Its Burst Frequency. To assess the causality of the suggested link between promoter acetylation state and burst frequency, we designed a system to modulate histone acetylation levels of a target promoter. To take advantage of a CRISPR/dCas9- and p300-based epigenome editing system, we used human HEK293T cells (29), into which we introduced a single copy of *Bmal1-sLuc2*, transcribed in large sporadic bursts (*SI Appendix*, Fig. S6*A*). Combined with dCas9 fused to the acetyltransferase domain of p300 (dCas9p300 WT), guide RNAs (gRNAs) specifically targeting the *Bmal1-sLuc2* reporter led to luciferase induction of up to threefold in a bulk-transfected population (*SI Appendix*, Fig. S6*B*). In contrast, gRNAs of scrambled sequences or dCas9 fused to an inactive p300 catalytic domain (dCas9p300 D1399Y) did not impact luciferase expression. To estimate the amount of dCas9p300 in each cell, we used a GFP marker of transfection efficiency and sorted cells displaying low (GFP−), high (GFP+), or very high (GFP++) levels of GFP (*SI Appendix*, Fig. S6*C*). In agreement with increased dCas9p300, cells with higher GFP levels showed increased histone acetylation of the *Bmal1-sLuc2* locus (Fig. 4*A*). We inferred the transcriptional bursting parameters corresponding to each condition from smRNA-FISH distributions (*SI Appendix*, Fig. S7 *A* and *B*). While cells in the least transfected dCas9p300 WT population and with inactive dCas9p300 contained an average of five transcripts per cell, cells in the active dCas9p300 GFP+ and GFP++ populations contained an average of 13 and 20 transcripts per cell, respectively (Fig. 4*B*). Interestingly, even though the bursting parameters of *Bmal1-sLuc2* were markedly different in the HEK293T cells compared with NIH 3T3 cells, this dCas9p300-mediated increase in mRNA expression arose principally from increased burst frequency

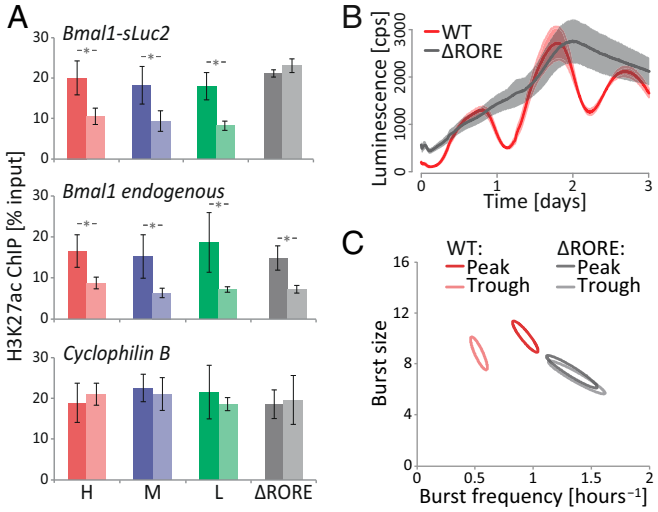

Fig. 3. Two ROREs responsible for rhythmic acetylation of the *Bmal1* promoter primarily modulate bursting frequency, but not burst size. (*A*) H3K27ac enrichment (ChIP-qPCR) at the *Bmal1-sLuc2* promoter (*Top*), endogenous *Bmal1* locus (*Middle*), and *Cyclophilin B* locus (*Bottom*) at *Bmal1-sLuc2* peak (dark) and trough (light) expression in the H, M, and L clones and a double ΔRORE mutant of the H clone (gray). Data are mean ± SD over three replicates. $*P < 0.05$, *t* test. (*B*) Effect of ΔRORE on *Bmal1-sLuc2* expression of the H clone on population-level real-time luminescence monitoring. Data are mean ± SD over three replicates. (*C*) Transcriptional bursting parameters for the ΔRORE mutant and control WT H clone inferred from *Bmal1-sLuc2* single-cell luminescence traces in time windows centered on the peak (10–22 h after dex synchronization) and trough (22–34 h after dex). Ellipses indicate the 95% CI of the posteriors.

SYSTEMS BIOLOGY

(Fig. 4*C*), since the burst size did not change significantly across all conditions (Fig. 4*D*). Thus, these data suggest that histone acetylation at the *Bmal1-sLuc2* promoter modulates transcriptional bursting by increasing the burst frequency.

H3K27ac and Burst Frequency Are Correlated for Other Clock-Dependent and -Independent Genes in Several Systems. We next assessed whether other rhythmically expressed genes similarly modulated their burst frequency rather than burst size, and if this phenomenon was also correlated with variation in histone acetylation. For this, we focused on the endogenous *Bmal1* and *Dbp* genes. While *Bmal1* is expected to behave like the luminescence reporter, *Dbp* is expressed antiphasically (*SI Appendix*, Fig. S8) and regulated by other factors (30). Here we used two-color intronic and exonic smRNA-FISH probes to quantify the number and intensity of active transcription sites (TSs), as well as the total number of cellular mRNAs (*SI Appendix*, Fig. S9*A*).

We first estimated the fraction of extrinsic transcriptional variability in our conditions, since the unbiased inference of transcriptional bursting parameters from smRNA-FISH via the negative binomial distribution requires low levels of extrinsic noise (4, 31). By computing the covariance of all pairs of TS intensities within the tetraploid NIH 3T3 cells (*SI Appendix*), we showed that the extrinsic noise accounted for 10–20% of the total noise in our smRNA-FISH system (*SI Appendix*, Fig. S9*B*). We then estimated transcriptional bursting parameters from the count distributions of mature transcripts as for *Bmal1-sLuc2* (*SI Appendix*, Fig. S9*C*). For both *Bmal1* and *Dbp*, circadian time significantly changed the burst frequency, which was higher at the respective peak expression times, while the burst size did not change significantly (Fig. 5*A*).

To substantiate these results, we also inferred the bursting parameters of the endogenous *Bmal1* and *Dbp* from the nascent transcript signals (*SI Appendix*, Fig. S9*D*). These analyses confirmed that burst frequency (in units of transcription elongation time) is higher at peak transcription for both genes, although the changes were greater than for mature transcripts (Fig. 5*B*). While the inferred burst sizes were similar and constant for cellular and nascent mRNAs for *Dbp*, *Bmal1* burst sizes were smaller for nascent transcripts and showed a slight temporal variation. Thus, while quantitatively the mature and nascent transcript approaches differ slightly, the consistent finding that changes in bursting frequency according to circadian time were more significant than changes in burst size was very robust.

We next assessed the acetylation states of *Bmal1* and *Dbp* promoters by H3K27ac ChIP-seq at peak and trough circadian expression levels. Although both genes displayed acetylation profiles with signal accumulating mainly at the TSS in *Bmal1* and within the gene body in *Dbp*, most of their H3K27ac peaks were reduced at the expression trough (Fig. 5*C*). Thus, as for *Bmal1-sLuc2*, the burst frequency of endogenous circadian genes also changed during the circadian period together with the promoter acetylation state, independent of the phase of expression and promoter *cis*-regulatory elements.

Finally, we tested whether histone acetylation correlated with burst frequency in other cell systems. We focused on a dataset of 38 mouse embryonic stem cell (mESC) genes with transcript counts per cell measured by smRNA-FISH (32). For each gene, the burst size and frequency were inferred from the mRNA distributions and transcript half-lives (33). The bursting parameters were then correlated with the enrichment of seven genomic marks in a 5-kb or 500-kb window around the TSSs and along the gene body (34). For both the 5-kb window and the gene body, among all genomic marks assessed, histone acetylation (H3K27ac and H3K9ac) was highly correlated with burst frequency (Fig. 5*D* and *SI Appendix*, Fig. S10*A*), indicating that hyperacetylated genes tend to have higher burst frequencies. This correlation was no longer present in the larger 500-kb window. However, no correlation could be detected between burst size and histone acetylation at any assessed genomic scale. Thus, while the correlation between active transcription and acetylation state is well known (35), our results suggest that this is caused by variations in burst frequency rather than by variations in burst size (*SI Appendix*, Fig. S10*B*).

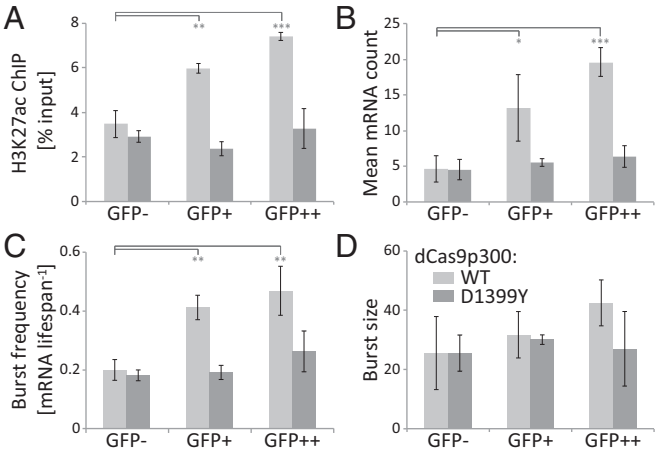

Fig. 4. Targeted histone acetylation of the *Bmal1-sLuc2* promoter increases burst frequency. (*A*) H3K27ac enrichment (ChIP-qPCR) at the *Bmal1-sLuc2* promoter. (*B–D*) Transcriptional bursting parameters inferred from negative binomial fits on *Bmal1-sLuc2* smRNA-FISH distributions: mean mRNA count per cell (*B*), burst frequency (*C*), and burst size (*D*). The sorted GFP–, GFP+, and GFP++ HEK293T cells contain increasing amounts of catalytically active (WT, light gray) or inactive (D1399Y, dark gray) dCas9p300. Data are mean ± SD over three replicates. **P* < 0.05; ***P* < 0.01; ****P* < 0.001, *t* test.

Discussion

Combining Approaches to Monitor Transcriptional Bursting. Measuring transcriptional bursting properties of a promoter is technically challenging, requiring quantitative measurements of expression product at single-gene resolution. Here we estimated the bursting parameters of the short-lived *Bmal1-sLuc2* reporter from protein levels in real time, from the distribution of mature transcripts in fixed cells and from the nascent transcripts at TSs. Each approach has pros and cons. Notably, in the live approach, transcription states are mathematically inferred from measured protein levels (23), while for smRNA-FISH distributions, the negative binomial fit assumes short bursts and negligible cell-to-cell variability (4, 19). Here we found that these strategies converged to similar results; the burst frequency was modulated over the circadian cycle, while the integration site mainly affected the burst size. This supports previous reports that the burst frequency and size are uncoupled and can be separately controlled to regulate expression levels (5, 11, 19, 20).

However, we also noticed quantitative differences between bursting parameters inferred using these various approaches. For example, smRNA-FISH tended to display lower amplitudes between circadian peaks and troughs compared with real-time luminescence or RNA time course analyses. Whether this resulted from imprecise estimations of the circadian times or technical limitations in the detection of transcripts remains unclear. Independent of the approach, the telegraph model only explains expression noise inherent to the gene activity (intrinsic noise) and may provide inaccurate estimations of the bursting parameters in the presence of significant extrinsic noise (36, 37). By using nondividing cells and controlling the circadian cycle, we minimized the levels of extrinsic noise in both real-time luminescence (23) and smRNA-FISH (*SI Appendix*, Fig. S9*B*) analyses. Additional efforts to decrease extrinsic noise levels could include the control of such factors as cell size (38, 39); however, even if the extrinsic noise remains low within an experimental condition, it may vary between biological replicates. Experimental variables, such as cell density or synchronization efficiency, can vary between replicates despite strict protocols and affect sensitive readouts, such as bursting parameters. Thus, while changes in bursting parameters within experiments performed

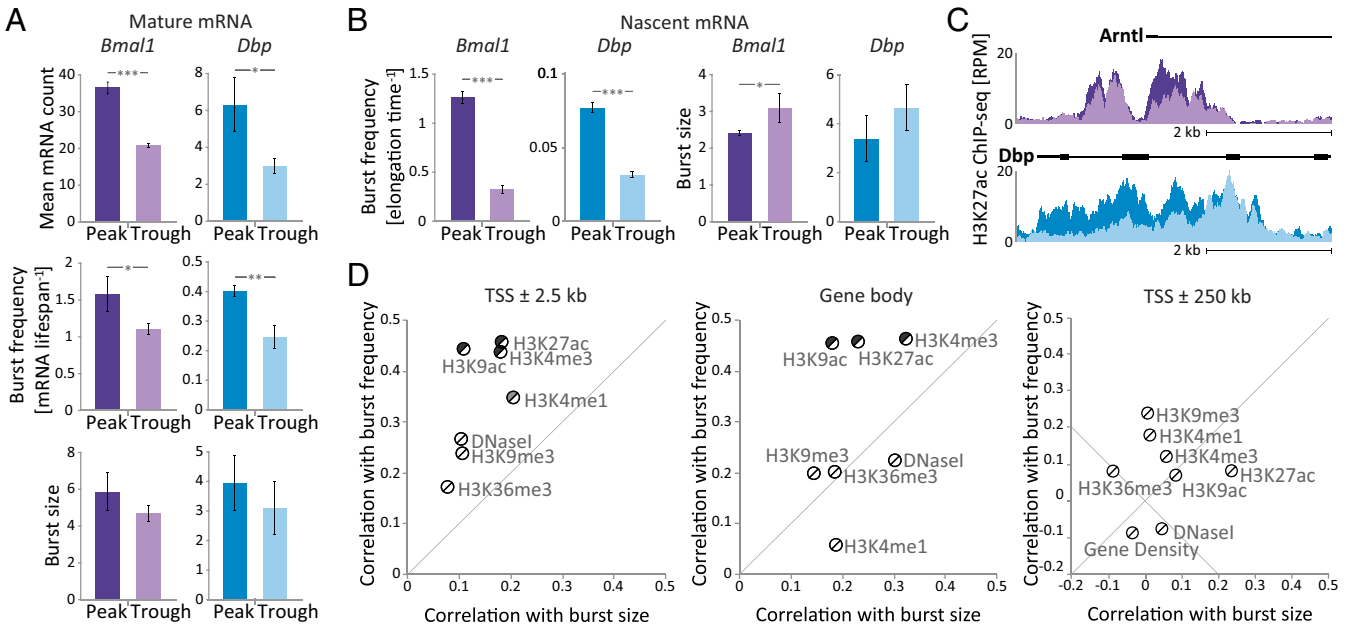

Fig. 5. The relationship between H3K27ac and burst frequency holds for other clock-dependent and -independent genes in different systems. (*A* and *B*) Transcriptional bursting parameters of endogenous *Bmal1* (purple) and *Dbp* (blue) inferred from negative binomial fits on smRNA-FISH mature transcript distributions (*A*) or from modeled nascent mRNA intensities at TSs (*B*) at expression peak (16 h and 30 h after dex for *Bmal1* and *Dbp*, respectively) or trough (28 h and 18 h). Data (mean mRNA count per cell, burst frequency and burst size) are mean ± SD over three replicates. $*P < 0.05$; $**P < 0.01$; $***P < 0.001$, *t* test. (*C*) H3K27ac ChIP-seq signal (in reads per million) around *Bmal1* (*Arntl*; purple) and *Dbp* (blue) TSSs. The dark and light density profiles correspond to H3K27ac enrichment at the expression peak (16 h and 28 h after dex for *Bmal1* and *Dbp*, respectively) and trough (28 h and 16 h). (*D*) Pearson correlation coefficients between genomic marks enrichment and burst size (*x*-axis) or burst frequency (*y*-axis) inferred from smRNA-FISH distributions of 38 mESC genes (32). The abundance of genomic marks was quantified in a 5-kb window around the TSS (*Left*), within the gene body (*Middle*), or in a 500-kb area around the TSS (*Right*). Shading intensity corresponds to significance of the correlation with burst frequency (above the diagonal) or burst size (below the diagonal). White, $P > 0.05$; gray, $P < 0.05$; black, $P < 0.01$, Pearson correlation.

at the same time appeared very robust, quantitative estimates of the bursting parameters remain challenging.

Histone Acetylation Determines the Burst Frequency. Here, by analyzing the bursting of a circadian gene, we found that histone acetylation levels modulate transcriptional burst frequency. In NIH 3T3 cells, H3K27ac levels at both WT and ΔRORE *Bmal1-sLuc2* promoters and in endogenous circadian genes covaried with the burst frequency. In a previous study, temporally averaged *Bmal1* burst frequency increased only marginally on drug-mediated histone hyperacetylation, because we did not stratify the analysis of bursting with respect to time (5). Similar links between H3K27ac levels and burst frequency were also observed in the *Cry1* gene in mouse liver, where burst frequency oscillated between the expression peak and trough together with enhancer-promoter contacts and histone acetylation (16). In addition, controlled increase of the *Bmal1-sLuc2* promoter acetylation levels in HEK293T cells by targeted p300 activity exclusively increased the burst frequency. Thus, promoter acetylation had a direct role in tuning the burst frequency, consistent with previous findings in yeast where deletion of most components of the acetylation machinery significantly reduced the burst frequency (40). While the bulk of our experiments were performed on *Bmal1-sLuc2*, the link between histone acetylation and burst frequency was also found in other systems, such as cell fate genes in mESCs. Thus, our correlative and functional analyses suggest that histone acetylation proximal to gene promoters may be a widespread determinant of burst frequency. The chromatin-loosening properties of histone acetylation could provide a possible explanation. Indeed, acetylated chromatin is more easily remodeled (41), and nucleosome density around TSSs has been shown to influence burst frequency (17, 19) as well as expression noise (42, 43), itself largely influenced by the burst frequency (44). Other known regulators of burst frequency, such as transcription factors or DNA looping, could be involved through active recruitment of the acetylation machinery (45), while the histone acetylation context reciprocally affects transcription factor binding and DNA looping formation by altering chromatin permissiveness.

Along with histone acetylation, other molecular mechanisms may influence burst frequency. Indeed, although in this study the promoter acetylation state was correlated with the burst frequency for many genes, counterexamples also exist (5, 21, 46). In conclusion, burst frequency is likely determined by a combination of factors, among which the promoter acetylation state plays a predominant role.

Unidentified Molecular Origins of the Burst Size. While the molecular determinants of the burst frequency are becoming clearer, the mechanisms influencing burst size remain largely unknown. In this study, we found that the integration sites of the reporters could change burst sizes, while the frequencies seemed less sensitive. Unfortunately, the limited number of integration sites available did not enable identification of the underlying discrepancies in burst sizes (*SI Appendix*, Fig. S5). Since none of the assessed histone marks correlated with burst size in a collection of 38 mESC genes (Fig. 5*D*), burst sizes may be influenced by combinations of factors or molecular states that are not captured by ChIP analysis of histone marks, such as transcription reinitiation. Notably, burst size could be influenced by the transient formation of gene clusters with enhanced transcription (47), as physical contacts with other active genes are good predictors of transcriptional output (48). These transcription domains could influence burst size by notably favoring the sharing of transcriptional machinery, such as RNA polymerase II (Pol II), between actively transcribing genes, as a reduction in Pol II level is sufficient to decrease burst size (39).

Materials and Methods

More detailed information on the materials and methods used in this study is provided in *SI Appendix*.

Cell Lines and Cell Culture. NIH 3T3-FRT cells were generated by transfecting a pFRT-Neo plasmid, and the presence of a single FRT site was verified by Southern blot analysis. Stable *Bmal1-sLuc2* NIH 3T3 clones H, M, and L were obtained by Flp/FRT recombination of a *Bmal1-sLuc2* expression vector. HEK293T cells stably expressing *Bmal1-sLuc2* were obtained from transduction of a pBmal1/NLS-luc lentivirus (5). Cells were maintained at 37 °C in a humid environment with DMEM complemented with 10% FBS.

Luminescence Recordings. The circadian clock was synchronized with dexamethasone before recording with an Actimetrics LumiCycle 32 (population) or LuminoView LV200 microscope (single-cell). Single-cell recordings were analyzed with the CAST platform (49).

Inferring Transcription Parameters from Single-Cell Luminescence Time-Traces. Luciferase protein and mRNA half-lives were estimated as described previously (5) from luminescence decay following actinomycin D or cycloheximide treatment. Likelihoods of individual time traces were calculated using a two-state telegraph model, with k_{on}, k_{off}, and k_m values estimated from Bayesian inference (23).

smRNA-FISH and Transcriptional Bursting Parameters Inference. smRNA-FISH was performed on serum-starved cells using Stellaris probes and imaged with a Leica DM5500B wide-field microscope. Transcripts were detected with CellProfiler on Z-projected stacks. Transcriptional bursting parameters were inferred from mature smRNA-FISH distributions (4, 19) or from nascent smRNA-FISH distributions using a Bayesian approach.

ChIP. ChIP analyses were performed using the MAGnify system. After sonication and immunoprecipitation, eluted samples were analyzed by quantitative PCR or by sequencing in an Illumina NextSeq 550 sequencing system.

dCas9p300-Mediated Epigenome Editing. HEK293T cells, for which the system was originally developed and optimized (29), were transiently transfected with dCas9p300 together with a GFP transfection efficiency marker and gRNAs. Cells were sorted accordingly to GFP intensity and analyzed by smRNA-FISH or ChIP.

Public Databases of Genomic Markers. Genomic features in 38 mESC genes was determined from public databases (34). Pearson correlation coefficients were calculated between the ChIP signals in different windows and bursting parameters inferred from previously published smRNA-FISH distributions (32).

ACKNOWLEDGMENTS. We thank Nick E. Phillips for his scientific input and Jürgen A. Ripperger for the pFRT-Neo plasmid. The computations were performed at Vital-IT (www.vital-it.ch). Work in the F.N. laboratory was supported by Swiss National Science Foundation Grant 31-153340; StoNets, a grant from the Swiss SystemsX.ch (www.systemsx.ch) initiative evaluated by the Swiss National Science Foundation; and the École Polytechnique Fédérale de Lausanne.

1. Larson DR (2011) What do expression dynamics tell us about the mechanism of transcription? *Curr Opin Genet Dev* 21:591–599.
2. Raj A, van Oudenaarden A (2008) Nature, nurture, or chance: Stochastic gene expression and its consequences. *Cell* 135:216–226.
3. Chubb JR, Trcek T, Shenoy SM, Singer RH (2006) Transcriptional pulsing of a developmental gene. *Curr Biol* 16:1018–1025.
4. Raj A, Peskin CS, Tranchina D, Vargas DY, Tyagi S (2006) Stochastic mRNA synthesis in mammalian cells. *PLoS Biol* 4:e309.
5. Suter DM, et al. (2011) Mammalian genes are transcribed with widely different bursting kinetics. *Science* 332:472–474.
6. Muramoto T, et al. (2012) Live imaging of nascent RNA dynamics reveals distinct types of transcriptional pulse regulation. *Proc Natl Acad Sci USA* 109:7350–7355.
7. Bahar Halpern K, et al. (2015) Bursty gene expression in the intact mammalian liver. *Mol Cell* 58:147–156.
8. Skinner SO, et al. (2016) Single-cell analysis of transcription kinetics across the cell cycle. *eLife* 5:e12175.
9. Nicolas D, Phillips NE, Naef F (2017) What shapes eukaryotic transcriptional bursting? *Mol Biosyst* 13:1280–1290.
10. Larson DR, et al. (2013) Direct observation of frequency-modulated transcription in single cells using light activation. *eLife* 2:e00750.
11. Senecal A, et al. (2014) Transcription factors modulate c-Fos transcriptional bursts. *Cell Rep* 8:75–83.
12. Xu H, Sepúlveda LA, Figard L, Sokac AM, Golding I (2015) Combining protein and mRNA quantification to decipher transcriptional regulation. *Nat Methods* 12:739–742.
13. Kafri P, et al. (2016) Quantifying β-catenin subcellular dynamics and cyclin D1 mRNA transcription during Wnt signaling in single living cells. *eLife* 5:e16748.
14. Bartman CR, Hsu SC, Hsiung CC-S, Raj A, Blobel GA (2016) Enhancer regulation of transcriptional bursting parameters revealed by forced chromatin looping. *Mol Cell* 62:237–247.
15. Fukaya T, Lim B, Levine M (2016) Enhancer control of transcriptional bursting. *Cell* 166:358–368.
16. Mermet J, et al. (2018) Clock-dependent chromatin topology modulates circadian transcription and behavior. *Genes Dev* 32:347–358.
17. Brown CR, Mao C, Falkovskaia E, Jurica MS, Boeger H (2013) Linking stochastic fluctuations in chromatin structure and gene expression. *PLoS Biol* 11:e1001621.
18. Dadiani M, et al. (2013) Two DNA-encoded strategies for increasing expression with opposing effects on promoter dynamics and transcriptional noise. *Genome Res* 23: 966–976.
19. Dey SS, Foley JE, Limsirichai P, Schaffer DV, Arkin AP (2015) Orthogonal control of expression mean and variance by epigenetic features at different genomic loci. *Mol Syst Biol* 11:806.
20. Dar RD, et al. (2012) Transcriptional burst frequency and burst size are equally modulated across the human genome. *Proc Natl Acad Sci USA* 109:17454–17459.
21. Wu S, et al. (2017) Independent regulation of gene expression level and noise by histone modifications. *PLoS Comput Biol* 13:e1005585.
22. Molina N, et al. (2013) Stimulus-induced modulation of transcriptional bursting in a single mammalian gene. *Proc Natl Acad Sci USA* 110:20563–20568.
23. Zoller B, Nicolas D, Molina N, Naef F (2015) Structure of silent transcription intervals and noise characteristics of mammalian genes. *Mol Syst Biol* 11:823.
24. Preitner N, et al. (2002) The orphan nuclear receptor REV-ERBalpha controls circadian transcription within the positive limb of the mammalian circadian oscillator. *Cell* 110: 251–260.
25. Akashi M, Takumi T (2005) The orphan nuclear receptor RORalpha regulates circadian transcription of the mammalian core-clock Bmal1. *Nat Struct Mol Biol* 12:441–448.
26. Yin L, Lazar MA (2005) The orphan nuclear receptor Rev-erbalpha recruits the N-CoR/histone deacetylase 3 corepressor to regulate the circadian Bmal1 gene. *Mol Endocrinol* 19:1452–1459.
27. Feng D, et al. (2011) A circadian rhythm orchestrated by histone deacetylase 3 controls hepatic lipid metabolism. *Science* 331:1315–1319.
28. Guillaumond F, Dardente H, Giguère V, Cermakian N (2005) Differential control of Bmal1 circadian transcription by REV-ERB and ROR nuclear receptors. *J Biol Rhythms* 20:391–403.
29. Hilton IB, et al. (2015) Epigenome editing by a CRISPR-Cas9-based acetyltransferase activates genes from promoters and enhancers. *Nat Biotechnol* 33:510–517.
30. Kiyohara YB, et al. (2008) Detection of a circadian enhancer in the mDbp promoter using prokaryotic transposon vector-based strategy. *Nucleic Acids Res* 36:e23.
31. Shahrezaei V, Swain PS (2008) Analytical distributions for stochastic gene expression. *Proc Natl Acad Sci USA* 105:17256–17261.
32. Singer ZS, et al. (2014) Dynamic heterogeneity and DNA methylation in embryonic stem cells. *Mol Cell* 55:319–331.
33. Sharova LV, et al. (2009) Database for mRNA half-life of 19 977 genes obtained by DNA microarray analysis of pluripotent and differentiating mouse embryonic stem cells. *DNA Res* 16:45–58.
34. Stamatoyannopoulos JA, et al.; Mouse ENCODE Consortium (2012) An encyclopedia of mouse DNA elements (Mouse ENCODE). *Genome Biol* 13:418.
35. Kuo M-H, Allis CD (1998) Roles of histone acetyltransferases and deacetylases in gene regulation. *BioEssays* 20:615–626.
36. Hilfinger A, Paulsson J (2011) Separating intrinsic from extrinsic fluctuations in dynamic biological systems. *Proc Natl Acad Sci USA* 108:12167–12172.
37. Swain PS, Elowitz MB, Siggia ED (2002) Intrinsic and extrinsic contributions to stochasticity in gene expression. *Proc Natl Acad Sci USA* 99:12795–12800.
38. Battich N, Stoeger T, Pelkmans L (2015) Control of transcript variability in single mammalian cells. *Cell* 163:1596–1610.
39. Padovan-Merhar O, et al. (2015) Single mammalian cells compensate for differences in cellular volume and DNA copy number through independent global transcriptional mechanisms. *Mol Cell* 58:339–352.
40. Weinberger L, et al. (2012) Expression noise and acetylation profiles distinguish HDAC functions. *Mol Cell* 47:193–202.
41. Verdone L, Agricola E, Caserta M, Di Mauro E (2006) Histone acetylation in gene regulation. *Brief Funct Genomic Proteomic* 5:209–221.
42. Small EC, Xi L, Wang J-P, Widom J, Licht JD (2014) Single-cell nucleosome mapping reveals the molecular basis of gene expression heterogeneity. *Proc Natl Acad Sci USA* 111:E2462–E2471.
43. Tirosh I, Barkai N (2008) Two strategies for gene regulation by promoter nucleosomes. *Genome Res* 18:1084–1091.
44. Munsky B, Neuert G, van Oudenaarden A (2012) Using gene expression noise to understand gene regulation. *Science* 336:183–187.
45. Fuda NJ, Ardehali MB, Lis JT (2009) Defining mechanisms that regulate RNA polymerase II transcription in vivo. *Nature* 461:186–192.
46. Harper CV, et al. (2011) Dynamic analysis of stochastic transcription cycles. *PLoS Biol* 9: e1000607.
47. Hnisz D, Shrinivas K, Young RA, Chakraborty AK, Sharp PA (2017) A phase separation model for transcriptional control. *Cell* 169:13–23.
48. Corrales M, et al. (2017) Clustering of *Drosophila* housekeeping promoters facilitates their expression. *Genome Res* 27:1153–1161.
49. Blanchoud S, Nicolas D, Zoller B, Tidin O, Naef F (2015) CAST: An automated segmentation and tracking tool for the analysis of transcriptional kinetics from single-cell time-lapse recordings. *Methods* 85:3–11.